

## COMMUNICATION

# A Sequential HNCA NMR Pulse Sequence for Protein Backbone Assignment

Axel Meissner and Ole Winneche Sørensen

Department of Chemistry, Carlsberg Laboratory, Gamle Carlsberg Vej 10, DK-2500 Valby, Denmark

Received December 14, 2000; revised March 7, 2001; published online April 17, 2001

**The conventional HNCA pulse sequence suffers from the ambiguity that it cannot distinguish inter- and intraresidue correlations because the one-bond and two-bond  $J(\text{NC}^\alpha)$  coupling constants are of similar magnitude. This paper presents a novel pulse sequence, *sequential*HNCA, that leads to a spectrum exhibiting exclusively interresidue correlations. This important sequential information has so far usually been obtained by an HN(CO)CA experiment that for medium field strengths typically also is more sensitive than HNCA. However, for increasing static magnetic fields the chemical shift anisotropy relaxation mechanism of carbonyl carbons becomes more and more efficient, leading to a degradation of the HN(CO)CA sensitivity. Hence there is a point where the *sequential* HNCA experiment becomes the most sensitive option for sequential N-C $^\alpha$  correlation.** © 2001 Academic Press

**Key Words:** multidimensional NMR; TROSY; sequential HNCA; sequential assignment; HN(CO)CA.

The assignment of the backbone resonances is a crucial step in NMR structure determination of  $^{13}\text{C}$ ,  $^{15}\text{N}$ -labeled proteins. One element of the experimental protocol is the correlation of  $^{15}\text{N}(i)$  with the intra-  $^{13}\text{C}^\alpha(i)$  and the interresidue  $^{13}\text{C}^\alpha(i-1)$ , where the latter is part of the sequential assignment. The experiment HNCA (1) and its various extensions deliver these two correlations in a single spectrum because the  $J$  coupling constants mediating the coherence transfers,  $^1J(\text{NC}^\alpha)$  and  $^2J(\text{NC}^\alpha)$ , are of similar magnitude. Hence the HNCA spectrum exhibits an ambiguity that needs to be resolved by another experiment. That is typically the HN(CO)CA experiment (1, 2) or variations thereof, where only the sequential correlations are observed. This selectivity is based on the fact that the  $^2J(\text{NC}^\alpha)$  coupling constant is too small for efficient coherence transfer so that the amide magnetization of  $^{15}\text{N}(i)$  can be channeled exclusively through the sequential  $^{13}\text{CO}(i-1)$  via  $^1J(\text{NC}^\alpha)$ .

A drawback of the otherwise unambiguous HN(CO)CA approach at high magnetic fields is the delays with transverse carbonyl carbon magnetization required for the  $\text{CO} \leftrightarrow \text{C}^\alpha$  transfers. Since the transverse relaxation rate of the carbonyl carbons

is dominated by the chemical shift anisotropy mechanism high fields are detrimental for the sensitivity of the experiment. There is an estimate in the literature (3) where a clear sensitivity advantage of HN(CO)CA over HNCA for the sequential correlations at 600 MHz is turned into a disadvantage at 900 MHz. It is not the purpose of this paper to theorize about the exact rotational correlation time or static magnetic field strength where the sensitivities are equal but rather to show how to resolve the ambiguity of conventional HNCA.

It is of interest to have an unambiguous way of correlating  $^{15}\text{N}(i)$  and  $^{13}\text{C}^\alpha(i-1)$  that avoids a period with transverse  $^{13}\text{CO}$  magnetization. That is accomplished with the new *sequential* HNCA pulse sequence outlined in Fig. 1. It is related to the conventional HNCA pulse sequence but modified to suppress the coherence transfer pathway involving magnetization transfer via the  $^1J(\text{NC}^\alpha)$  coupling constant. An alternative modified HNCA experiment by Permi and Annala (4) introduces different multiplet structures of inter- and intraresidual peaks in the same spectrum allowing to distinguish the two types of correlations in that way.

The basic idea is related to a feature of experiments for determination of relative signs of coupling constants (5): Introduce the  $I_z(^{13}\text{CO})$  operator via  $^1J(\text{NC}^\alpha)$  and  $^{15}\text{N}$  magnetization, and remove it via  $^1J(\text{C}^\alpha\text{C}^\alpha)$  and  $^{13}\text{C}^\alpha$  magnetization. This works fine for the sequential correlation via  $^2J(\text{NC}^\alpha)$ , e.g.,

$$\begin{aligned} I_y[^{15}\text{N}(i)] &\rightarrow 4I_y[^{15}\text{N}(i)]I_z[^{13}\text{C}^\alpha(i-1)]I_z[^{13}\text{CO}(i-1)] \\ &\rightarrow 4I_z[^{15}\text{N}(i)]I_y[^{13}\text{C}^\alpha(i-1)]I_z[^{13}\text{CO}(i-1)] \\ &\rightarrow 2I_z[^{15}\text{N}(i)]I_x[^{13}\text{C}^\alpha(i-1)] \\ &\rightarrow 2I_y[^{15}\text{N}(i)]I_z[^{13}\text{C}^\alpha(i-1)] \\ &\rightarrow I_x[^{15}\text{N}(i)], \end{aligned} \quad [1a]$$

where the boldface arrows indicate  $J$  evolution and the smaller arrows a pair of  $^{15}\text{N}$  and  $^{13}\text{C}^\alpha$   $\pi/2$  pulses.

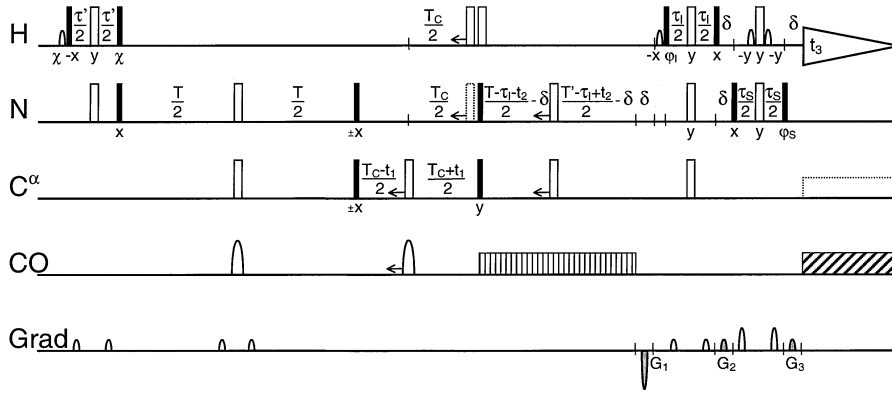


**FIG. 1.** *Sequential HNCA pulse sequence.* For Bruker instruments, phases  $\phi_1 = -y$ ,  $\phi_S = -y - \Delta\phi_S$  and gradient ratios  $(G_1 : G_2 : G_3) = (-7 : 3 : 1.987)$  select the echo, whereas the setting  $\phi_1 = y$ ,  $\phi_S = y - \Delta\phi_S$  and  $(G_1 : G_2 : G_3) = (-8 : 2 : 3.013)$  selects the antiecho. On Varian instruments the  $\phi_1$  and  $\phi_S$  phases must be inverted. In order to include the native  $^{15}\text{N}$  magnetization,  $\chi$  is  $y$  and  $-y$  on Bruker and Varian instruments, respectively. The prefix “ $\pm$ ” to pulse phases indicates independent  $\pi$  phase shift two-step cycles with alternating receiver phase. All delays  $\tau$  are on the order of  $(2J_{\text{NH}})^{-1}$ ;  $\tau_1$  and  $\tau_S$  can be adjusted according to *clean* TROSY (6) while  $\tau'$  typically is slightly shorter than  $(2J_{\text{NH}})^{-1}$  to compensate decay by transverse relaxation.  $\delta$  is a gradient delay.  $T$  is adjusted for optimum transfer between  $^{15}\text{N}$  and  $^{13}\text{C}^\alpha$  via the  $^2J(\text{NC}^\alpha)$  coupling constant while  $T_C$  is the usual compromise for  $^1J(\text{C}'\text{C}^\alpha)$  evolution while not allowing excessive  $^1J(\text{C}^\alpha\text{C}^\beta)$  evolution (see Figs. 2 and 3 captions). Water-selective  $\pi/2$  pulses serving to avoid saturating the water resonance are indicated.

The corresponding intra-residual pathway via  $^1J(\text{NC}^\alpha)$  is, e.g.,

$$\begin{aligned}
 I_y[^{15}\text{N}(i)] &\rightarrow 4I_y[^{15}\text{N}(i)]I_z[^{13}\text{C}^\alpha(i)]I_z[^{13}\text{CO}(i-1)] \\
 &\rightarrow 4I_z[^{15}\text{N}(i)]I_y[^{13}\text{C}^\alpha(i)]I_z[^{13}\text{CO}(i-1)] \\
 &\rightarrow 8I_z[^{15}\text{N}(i)]I_x[^{13}\text{C}^\alpha(i)]I_z[^{13}\text{CO}(i-1)]I_z[^{13}\text{CO}(i)] \\
 &\rightarrow 8I_y[^{15}\text{N}(i)]I_z[^{13}\text{C}^\alpha(i)]I_z[^{13}\text{CO}(i-1)]I_z[^{13}\text{CO}(i)] \\
 &\rightarrow 4I_x[^{15}\text{N}(i)]I_z[^{13}\text{CO}(i-1)]I_z[^{13}\text{CO}(i)]. \quad [1b]
 \end{aligned}$$

The last term in expression [1b] will not lead to observable magnetization because the  $J(\text{NC}')$  couplings are suppressed during the rest of the pulse sequence. Even without  $^{13}\text{CO}$  decoupling during acquisition the term would be unobservable because  $^2J(\text{NC}')$  vanishes. Thus the intraresidual correlation is suppressed.

The *sequential* HNCA pulse sequence outlined in Fig. 1 includes a *clean* TROSY element (6) for the final transfer of magnetization from  $^{15}\text{N}$  to the attached protons but the scheme for suppression of intraresidual correlations is independent of what element is used for  $^{15}\text{N} \rightarrow ^1\text{H}$  magnetization transfer.

In contrast to the conventional HNCA experiment obtained by omitting the first  $^{13}\text{CO}$   $\pi$  pulse, displacing the second by  $T_C/2$  to the right, and changing the phase of the second  $^{15}\text{N}$   $\pi/2$  pulse by  $90^\circ$ , the intensity in *sequential* HNCA is for the pertinent peaks multiplied by  $\sin[\pi^1J(\text{NC}')T] \sin[\pi^1J(\text{C}'\text{C}')T_C]$ . The sign of this product reflects the relative signs of the two  $J$  coupling constants involved.

There are a few additional technical details of the pulse sequence in Fig. 1 to mention. The  $\pi(^1\text{H})$  pulse in the  $t_1$  period serves to suppress  $^1J(\text{C}^\alpha\text{H}^\alpha)$  but since it also interchanges

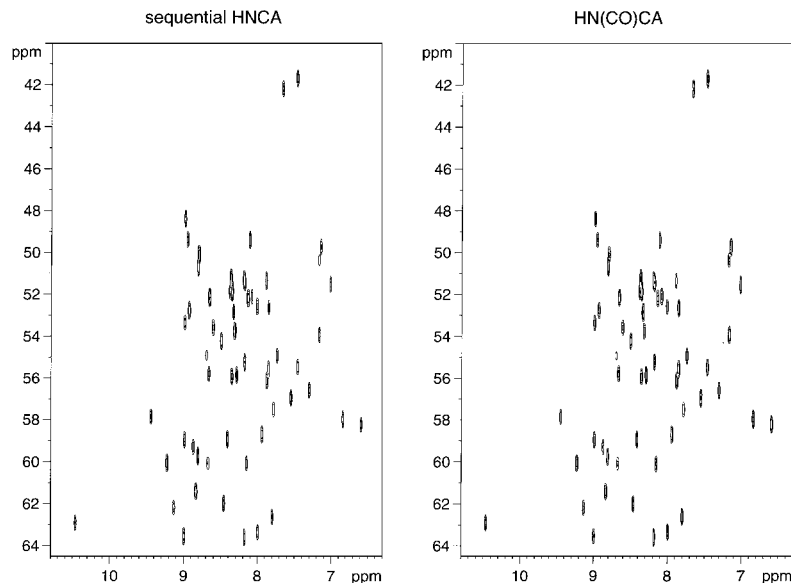
TROSY and anti-TROSY resonances in the  $^{15}\text{N}-^1\text{H}$  segments a second  $\pi(^1\text{H})$  pulse is included at the end of the  $t_1$  period. This pair of  $\pi(^1\text{H})$  pulses would be replaced by multipulse deuterium decoupling during  $^{13}\text{C}^\alpha$  evolution in perdeuterated proteins. The dotted  $\pi(^{15}\text{N})$  pulse in the  $t_1$  period can be considered optional since  $T_C$  is so short that there is no appreciable evolution due to  $J(\text{NC}^\alpha)$  coupling constants.

Figure 2 verifies by 2D projections of 800 MHz spectra of Chymotrypsin Inhibitor 2 (7, 8) that the same (sequential) correlations are observed in *sequential* HNCA and in HN(CO)CA. It is also noteworthy that the relative intensities within the two spectra are similar.

In Fig. 3, the 2D *sequential* HNCA spectrum is held up against a conventional HNCA spectrum exhibiting both intra- and inter-residual correlation peaks. Finally, the figure also shows a linear combination where the two spectra are subtracted from each other to yield an exclusive intraresidual HNCA correlation spectrum. If both the conventional and the *sequential* HNCA spectra are recorded it requires more instrument time. Nevertheless, this seems the way of choice for large molecules at high fields where the sensitivity of HN(CO)CA is unattractive. Since the sequential correlations are weaker than the intraresidual ones the overall sensitivity increases if more scans are recorded for *sequential* HNCA than for conventional HNCA. Ideally the signal-to-noise ratio for the weakest signals of interest should be the same in the two edited spectra.

Although there are variations in the  $J(\text{NC}^\alpha)$  coupling constants the editing of the intraresidual correlations is rather clean as can be seen from the sections in Fig. 4 taken from the framed regions in Fig. 3.

In conclusion, we have introduced a new pulse sequence, *sequential* HNCA, for correlation of  $^{15}\text{N}(i)$  with interresidue



**FIG. 2.** Comparison of excerpts from the first  $t_2$  interferogram (echo) of the  $C^\alpha$  region of *sequential* HNCA and HN(CO)CA TROSY experiments, respectively of  $^{15}\text{N}$ ,  $^{13}\text{C}$ -labeled CI2 21-83 (90%  $\text{H}_2\text{O}/10\%\text{D}_2\text{O}$ ,  $25^\circ\text{C}$ , pH 4.2, 4.18 mM). The *sequential* HNCA spectrum (left) was recorded with the pulse sequence in Fig. 1 on a Varian Unity Inova 800 MHz spectrometer. Parameters: relaxation delay 1.5 s;  $\tau' = \tau_1 = \tau_S = 5.43$  ms;  $T = 22.00$  ms;  $T' = 21.00$  ms;  $T_C = 7.60$  ms;  $\delta = 1.10$  ms;  $t_1(\text{max}) = 7.28$  ms; 64 scans. Sinc-shaped (9) selective  $\pi/2$  water pulses (1000.0  $\mu\text{s}$ ) and iBurp-shaped (10) selective carbon  $\pi$  pulses (930.0  $\mu\text{s}$ ) were used. Rectangular  $\pi/2$  and  $\pi$   $C^\alpha$  pulses were calibrated to have a zero excitation profile in the CO region. Adiabatic decoupling of CO during  $^{15}\text{N}$  constant time evolution covering 20 ppm was applied using WURST-2 decoupling (11); GARP decoupling (12) was used during data acquisition. The gradients in the self-compensating pairs had relative amplitudes of 1.0 in the initial INEPT transfer, 0.5 in the  $T$  periods, 1.0 in the first  $\text{S}^3\text{CT}$  element of TROSY transfer, and 6.0 in the final  $\text{S}^3\text{CT}$ /Watergate element. Data matrices of  $84 \times 2048$  points covering  $5632 \times 12,000$  Hz were zero-filled to  $1024 \times 2048$  prior to Fourier transformation and the window function was cosine in both dimensions. A modified HN(CO)CA TROSY (1, 2) was recorded (right) with the same parameters except for an  $\text{N} \leftrightarrow \text{CO}$  transfer delay of 33.30 ms; a delay for  $\text{CO} \leftrightarrow C^\alpha$  transfer of 8.90 ms; and a delay for constant-time  $C^\alpha$  evolution of 7.6 ms. Proton decoupling and the TROSY mixing sequence with gradients were as shown in Fig. 1. Adiabatic decoupling of  $C^\alpha$  during  $^{15}\text{N}$  constant-time evolution covering 20 ppm was applied using WURST-2 decoupling.

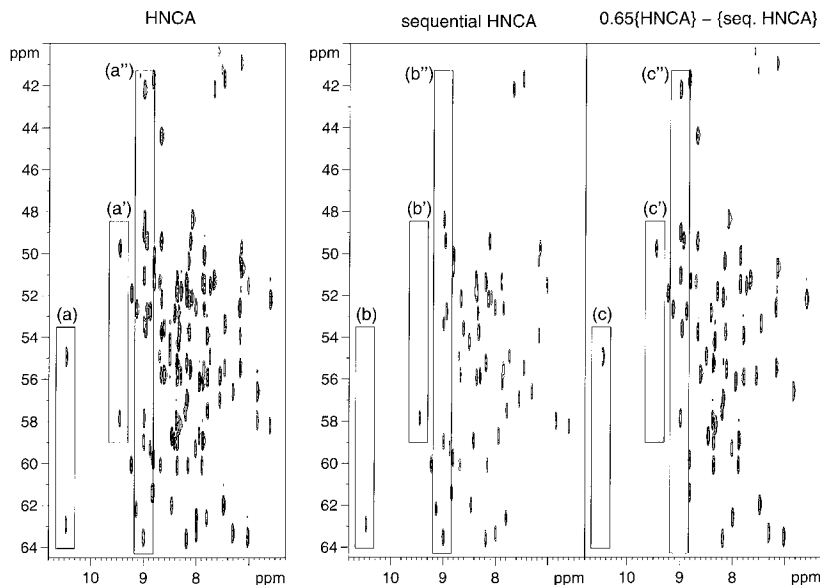


**FIG. 3.** HNCA TROSY (left), *sequential* HNCA (middle) and edited intraresidual HNCA (right) spectra of  $^{15}\text{N}$ ,  $^{13}\text{C}$ -labeled CI2 21-83 (90%  $\text{H}_2\text{O}/10\%\text{D}_2\text{O}$ ,  $25^\circ\text{C}$ , pH 4.2, 4.18 mM). The HNCA TROSY spectrum was recorded with the pulse sequence in Fig. 1 where the first shaped CO  $\pi$  pulse was omitted and the second CO  $\pi$  pulse displaced to be simultaneous with the  $^1\text{H}$  and  $^{15}\text{N}$   $\pi$  pulse within the  $C^\alpha$  constant-time period. The phase of the second  $^{15}\text{N}$   $\pi/2$  pulse was  $\pm y$ . Same parameters were used as listed in the Fig. 2 caption for *sequential* HNCA. The intraresidual HNCA spectrum, showing only HNCA correlations within the same amino acid, was obtained by linear combination of HNCA TROSY and *sequential* HNCA in a ratio of  $0.65 : -1$ .  $F_1$  traces along the center of the boxes in the spectra are shown in Fig. 4.

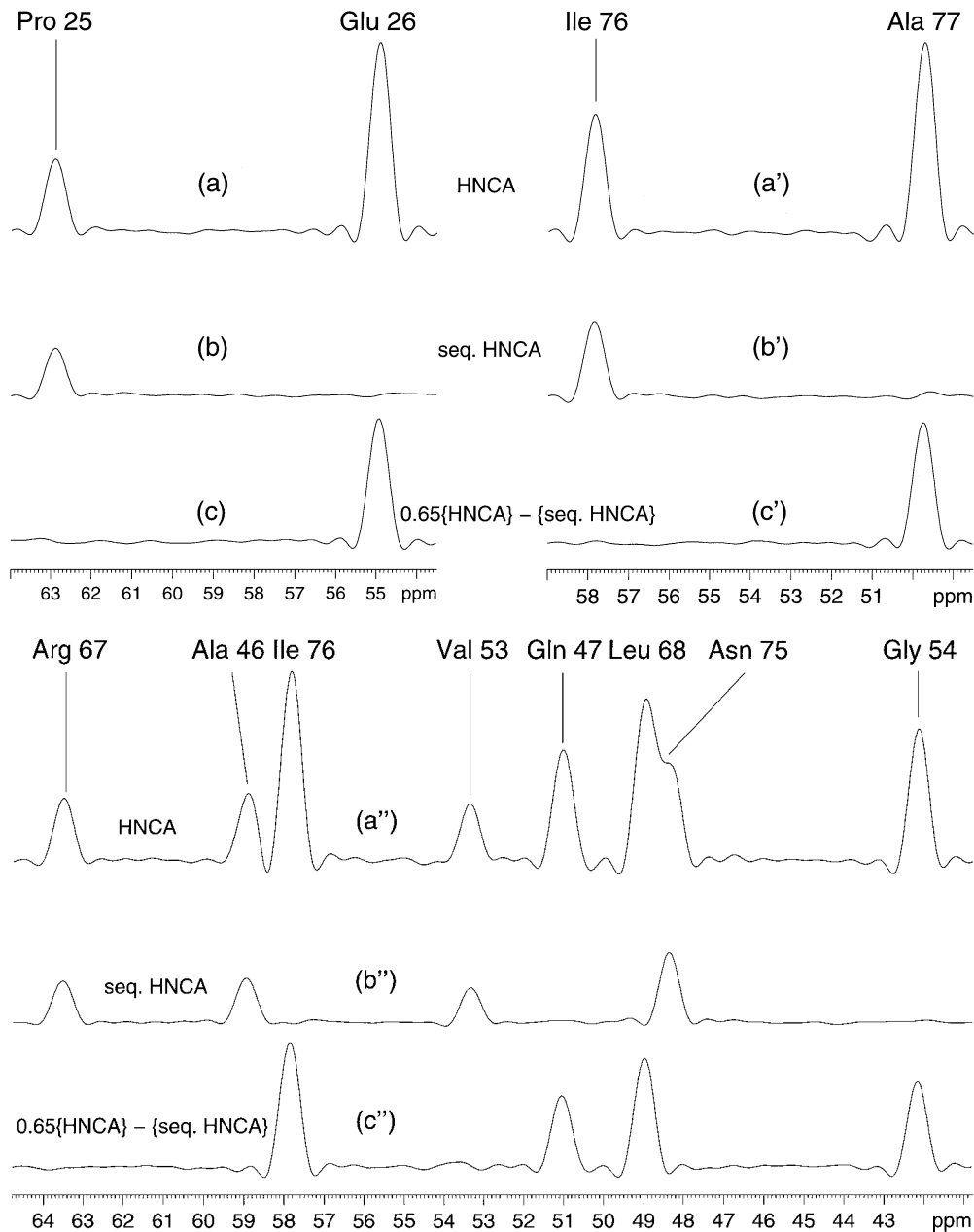


**FIG. 4.** 1D sections along the center of the boxes as indicated in Fig. 3. (a), (a'), and (a'') HNCA TROSY where both sequential ( $H_{(i)} - C_{(i-1)}^\alpha$ ) and intraresidual ( $H_{(i)} - C_{(i)}^\alpha$ ) correlations are present. (b), (b'), and (b'') *Sequential* HNCA TROSY showing only the sequential ( $H_{(i)} - C_{(i-1)}^\alpha$ ) correlations. (c), (c'), and (c'') Linear combination of HNCA TROSY and *sequential* HNCA in the ratio 0.65 : -1 yielding the spectrum containing only intraresidual ( $H_{(i)} - C_{(i)}^\alpha$ ) correlations.

$^{13}\text{C}^\alpha(i-1)$  in large proteins at high fields. The technique can be extended to other experiments benefiting from unambiguous magnetization transfer between  $^{15}\text{N}(i)$  and  $^{13}\text{C}^\alpha(i-1)$ .

Poulsen, Pia Skovgaard, and Mathilde H. Lerche for the  $^{15}\text{N}$ ,  $^{13}\text{C}$ -labeled C12 sample.

#### ACKNOWLEDGMENT

The spectra presented were recorded on the Varian Unity Inova 800 MHz spectrometer of the Danish Instrument Center for NMR Spectroscopy of Biological Macromolecules at Carlsberg Laboratory. We thank Flemming M.

#### REFERENCES

1. L. E. Kay, M. Ikura, R. Tschudin, and A. Bax, *J. Magn. Reson.* **89**, 496–514 (1990).
2. M. Salzmann, G. Wider, K. Pervushin, H. Senn, and K. Wüthrich, *J. Am. Chem. Soc.* **121**, 844–848 (1999).

3. J. P. Loria, M. Rance, and A. G. Palmer III, *J. Magn. Reson.* **141**, 180–184 (1999).
4. P. E. Permi and A. J. Annala, *J. Biomol. NMR*, in press.
5. O. W. Sørensen and R. R. Ernst, *J. Magn. Reson.* **63**, 219–224 (1985).
6. T. Schulte-Herbrüggen and O. W. Sørensen, *J. Magn. Reson.* **144**, 123–128 (2000).
7. P. Osmark, P. Sørensen, and F. M. Poulsen, *Biochemistry* **32**, 11007–11014 (1993).
8. J. C. Madsen, O. W. Sørensen, P. Sørensen, and F. M. Poulsen, *J. Biomol. NMR* **3**, 239–244 (1993).
9. A. J. Temps and C. F. Brewer, *J. Magn. Reson.* **56**, 355–372 (1984).
10. H. Geen and R. Freeman, *J. Magn. Reson.* **93**, 93–141 (1991).
11. E. Kupce and G. Wagner, *J. Magn. Reson. Ser. B* **109**, 329–333 (1995).
12. A. J. Shaka, P. B. Barker, and R. Freeman, *J. Magn. Reson.* **64**, 547–552 (1985).